Steady-State Drop-Size Distributions in High Holdup Fraction Dispersion Systems

E. G. Chatzi and C. Kiparissides
Chemical Engineering Dept. and Chemical Process Engineering Research Institute,
Aristotle University of Thessaloniki, Thessaloniki, Greece

Macroscopic phenomena in suspension polymerization reactors are extremely complex, and breakage and coalescence of polymerizing monomer droplets are not well understood, especially for high dispersed-phase volume fractions. Depending on the agitation, concentration and type of surface-active agent, the droplet size can exhibit a U shape variation with respect to the impeller speed. This behavior has been confirmed experimentally and theoretically as the balance between breakage and coalescence rates of monomer drops. Both processes are related to the drop surface energy, which is proportional to the interfacial tension and its variation with time. In this study, the most comprehensive models describing breakage and coalescence processes in a dispersion system were incorporated into a generalized numerical algorithm to predict the steady-state drop-size distributions in a high holdup (50%) liquid-liquid dispersion system. To assess the effectiveness of the theoretical model in simulating drop-size distributions in high holdup dispersion systems, experiments were carried out with a model system of 50% n-butyl chloride in water in the presence of a surface-active agent, poly(vinyl alcohol), at different concentrations and agitation rates. The theoretical model can predict reasonably well the drop-size distribution for all experimental conditions. A systematic theoretical and experimental investigation elucidates the relationships between the changing structure of PVA molecules at the monomer/water interface and their effects on breakage and coalescence frequencies at different agitation times and rates.

Introduction

The droplet-size distribution of a liquid-liquid dispersion in an agitated vessel is controlled by two dynamic processes: namely, the drop breakage and the drop coalescence. Droplet formation in the initial period of mixing as well as the dynamic equilibrium between drop breakage and coalescence are determined by the hydrodynamic conditions in the vessel and the physical properties of the system. For a low-coalescence system, parameters such as high impeller speed or low interfacial tension generally increase the droplet breakage frequency. On the other hand, for a high-coalescence system, if coalescence is caused by the drainage of the intervening film between two deformable colliding drops, then a high impeller speed or/and a low interfacial tension result in a decrease of the coalescence efficiency. For drops behaving as rigid spheres, which is typical for drops with small diameters or high interfacial tension, coalescence efficiency is independent of interfacial tension and increases with impeller speed. On the contrary, if coalescence takes place upon droplet impact (the turbulent energy of collision of the drops is greater than their total surface energy), a low interfacial tension and a high impeller speed cause an increase of the drop coalescence efficiency.

The influence of the large-scale flow on the drop breakage and coalescence processes may be considered comparatively small, since these phenomena occur in a microscale: they are determined by what happens in a small volume of fluid surrounding the individual droplet. Thus, if the Reynolds number of the main flow is high, the droplet interaction processes can be estimated using the theoretical developments of local isotropy. Homogeneous interaction models have been extensively used in the literature for the description of lean liquid-liquid dispersions in agitated vessels. They are based on the

Correspondence concerning this article should be addressed to C. Kiparissides.

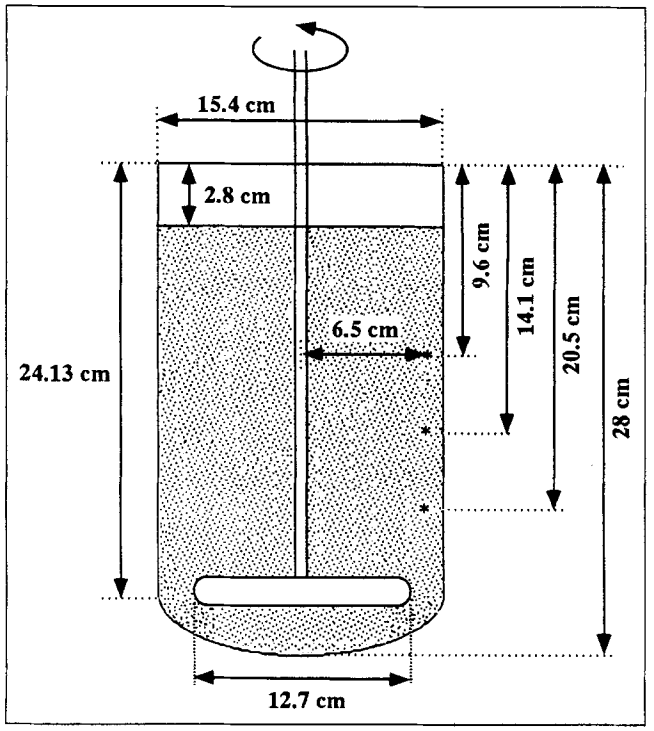

Figure 1. Geometrical characteristics of the mixing vessel.

assumptions of perfect macromixing and statistical homogeneity of the vessel content. In the present investigation, the homogeneous interaction model developed by Valentas and Amundson (1966) was employed to simulate the experimentally measured steady-state drop-size distributions obtained in a 1-gal (3.8-L) reactor provided with a flat-paddle impeller. The liquid-liquid dispersion system consisted of 50% *n*-butyl chloride in water containing a poly(vinyl alcohol) (PVA) surface active agent with a hydroxyl group content of 73 mol %. For the specific geometric and agitation characteristics of the vessel, it was found experimentally that the assumption of spatial homogeneity held true. This does not necessarily imply that the turbulence and energy conditions were uniform throughout the vessel, but since it was very difficult to estimate the local variations of flow, energy conditions, and droplet interaction frequencies in the vessel, they were considered uniform for modeling purposes.

Droplet-size Distribution Measurements

The stirred vessel used was a one-gallon stainless-steel round-bottomed ASME code stamped Chemineer unbaffled reactor with a 15.2-cm internal diameter and a 24.1-cm straight side. The reactor was equipped with a two-bladed flat impeller with a 12.7-cm dia. (Figure 1). In all experiments the volume of the dispersion was 4,464 cm^3. The bench-scale reactor system has been built to accommodate vinyl free-radical suspension polymerization reactions, and comprised the following interconnected units: the reactor unit, the heating and cooling unit, the feed unit, the steam generation unit, the sampling unit, the vacuum unit, the reaction termination unit, the process panel, and the supervisory process computer and interface (Voutetakis, 1992).

To investigate the effect of process parameters (impeller speed, type and concentration of stabilizer) on the droplet and particle-size distribution in vinyl monomer suspension polymerization reactions at low conversions, a series of experiments was carried out using a model liquid-liquid dispersion system of *n*-butyl chloride in water. An in-line sampling technique was developed to obtain representative samples of the dispersion from different locations in the reactor. A stainless-steel tube with a 0.63-cm ID fitted with a two-way stainless-steel ball valve was placed at specific positions inside the reactor. Samples were withdrawn from three locations set 6.5 cm from the impeller axis and 6.8, 11.3 and 17.7 cm from the free surface of the dispersion.

Several experiments were carried out with a 50% volume fraction of *n*-butyl chloride (Merck) in water at atmospheric pressure and a constant temperature of 20°C. The impeller speed was varied from 400 to 700 rpm. The continuous aqueous phase contained PVA of various concentrations (0.5–1 g/L), having a weight-average molecular weight of 76,000 and a number-average molecular weight of 19,000. The degree of hydrolysis was 72.5 mol % and the average VOH and VAc sequence lengths were 6.9 and 2.6, respectively. The various experimental conditions are shown in Table 1. A steady-state

Table 1. Experimental Conditions and Model Parameters

Temp. (°C)	Φ	Impeller Speed (rpm)	PVA Conc. (g/L)	$S_X \times 10^{-7}$	$S_{Nsa} \times 10^{-7}$	N_{da}	$C_1 \times 10^{-9}$	C_{VIII}	$C_{VI} \times 10^4$	$C_V \times 10^8$
20	0.5	400	0.5	5	4	5	70	0.6	1	1
20	0.5	450	0.5	5	4	5	35	0.6	1	1
20	0.5	500	0.5	5	4	5	20	0.6	1	1
20	0.5	550	0.5	5	4	5	8	0.6	1	1
20	0.5	600	0.5	5	4	5	4	0.6	1	1
20	0.5	650	0.5	5	4	5	2	0.6	1	1
20	0.5	700	0.5	5	4	5	0.7	0.6	1	1
20	0.5	400	1	5	4	5	70	0.6	1	1
20	0.5	450	1	5	4	5	35	0.6	1	1
20	0.5	500	1	5	4	5	20	0.6	1	1
20	0.5	550	1	5	4	5	8	0.6	1	1
20	0.5	600	1	5	4	5	4	0.6	1	1
20	0.5	650	1	5	4	5	2	0.6	1	1
20	0.5	700	1	5	4	5	0.7	0.6	1	1

drop-size distribution was achieved in less than 90 min for all experimental conditions investigated.

The time evolution of the interfacial tension between the *n*-butyl chloride phase and the aqueous PVA solution was measured by a Kruss surface tensiometer, model K10, using the Wilhelmy plate method. The experimental procedure recommended by the manufacturer was closely followed for each measurement. For the calibration of the instrument, the plate attached to the measuring torsion balance was initially submerged into a sample vessel containing the *n*-butyl chloride. Subsequently, the plate was removed from the *n*-butyl chloride container and carefully cleaned and annealed. Then, a second vessel containing the aqueous PVA solution was raised against the bottom edge of the plate until it became moistened. Finally, the light *n*-butyl chloride phase was carefully poured over the heavier aqueous phase so that the plate remained submerged at the same depth as it was during calibration. The value of interfacial tension was recorded at different times until the system reached equilibrium. It should be pointed out that interfacial tension measurements were collected until the gradient of the surface tension with respect to time was less than 0.01.

The experimental procedure followed for all droplet-size distribution measurements included the following steps.

1. Initially the system was thoroughly degreased and cleaned with distilled water.
2. The vessel was subsequently filled with the required amount of distilled water, a concentrated PVA solution, and the appropriate amount of *n*-butyl chloride up to a total volume of 4,464 cm^3. The reactor temperature was maintained at a constant value (20°C) and the impeller speed was adjusted to the desired setting.
3. The reactor was then positively pressurized at 5 psig (34 kPa) by charging a small amount of nitrogen gas into the reactor head space.
4. At prespecified time intervals, the ball valve of the sampling line was turned on to withdraw approximately 5 cm^3 of dispersion into 450 cm^3 of a concentrated PVA solution (10 g/L). The stabilized and diluted sample was immediately transferred to a small volume stirred cell of a laser diffraction particle sizer for measuring the droplet-size distribution. The sampling system (tubing and measuring-cell) was thoroughly cleaned before each measurement. Note that the first 10–15 mL of each sample withdrawn from the reactor were discarded in order to minimize the effect of stagnant dispersion fluid in the sampling tubes.

Several sampling and measuring procedures were tested in order to ensure that the measured sample was representative of the actual distribution in the reactor. To overcome any problems related to the pumping of the liquid dispersion, samples were collected through an immersed sampling tube by applying positive pressure. The sample was directly introduced into a dilution vessel containing a predetermined quantity of concentrated PVA solution (10 g/L). The dilution vessel as well as the measuring cell were gently stirred by Teflon-covered magnetic stirrers to avoid droplet flocculation as well as deformation and breakage of the drops. It is important to notice that measurements of the droplet-size distribution of different samples collected from the dilution vessel did not show any significant changes over a period of 20 min. Finally, the reproducibility of the experimental procedure is demonstrated in Figure 2. These curves represent the measured steady-state drop-size distributions in two different experiments under identical conditions.

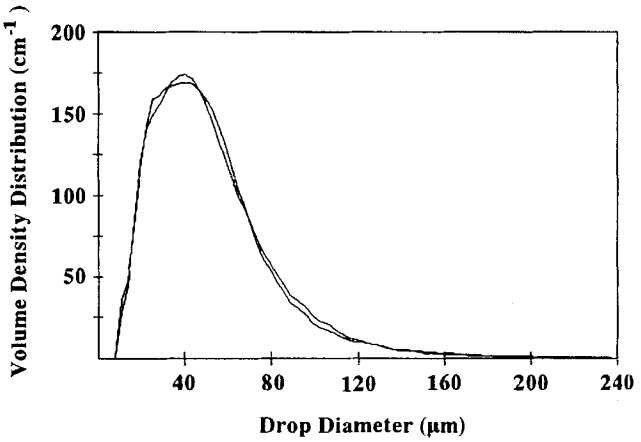

Figure 2. Reproducibility of the experiments (steady-state drop-size distribution at [PVA]=0.5 g/L and 700 rpm).

The drop-size distributions were measured by a Malvern laser diffraction particle sizer, model 2605c, based on Fraunhofer diffraction and interfaced with an Olivetti M24 microcomputer. A lens with a focal length of 300 mm and a dynamic range 180:1 was attached to the optical measurement unit. The analyzer was capable of detecting droplets in the size range of 5.8–564 μm with an accuracy of $\pm 4\%$ on the volume median diameter. The particle-size volume frequencies are extracted from the diffraction pattern by performing an iterative nonlinear least-squares calculation starting from the raw data and using a model-independent initial distribution. In this way, bimodal particle-size distributions can be identified with high resolution (Bürkholz and Polke, 1984). The primary output of the instrument was the relative volume-size distribution stored in 32 size classes uniformly spaced on a logarithmic scale.

Typical results generated by the instrument included cumulative size distribution, volume fraction within each size band, and a listing of the main parameters of the distribution, including the volume mean, median, and Sauter mean diameter. A computer program was developed for the mathematical transformation of the measured volume frequency distributions to corresponding volume density and diameter density distributions. Thus the discrete distributions could be transformed into continuous ones using a quasi-cubic Hermite splines method. Various characteristic moments and averages of the discrete distributions such as expected drop diameter, surface and arithmetic means, maximum diameter, as well as the total number of drops in the vessel could be calculated from the measured volume frequency data.

Experimental Results

Vessel homogeneity

In general, even a fully developed turbulent flow field in an agitated vessel is far from homogeneous. For example, significant differences can exist between the dispersed phase interactions in the impeller and circulation regions. It has been

postulated in the literature that the impeller region is dominated by drop breakage and the circulation region by drop coalescence. However, since it is difficult to estimate the local variations of interaction frequencies in an agitated vessel, the applicability of inhomogeneous interaction models is rather limited. For simulation purposes the homogeneous interaction models are often used, which neglect the local variations of flow, energy conditions and interaction frequencies, thus, assuming perfect macromixing and statistical homogeneity. Perfect macromixing implies that any differential volume element is representative of the vessel content, and statistical homogeneity means that the time average position distributions of drops in any two differential volumes in the vessel are approximately the same.

The validity of the spatial homogeneity assumption regarding the drop-size distribution of a dispersion depends on the experimental conditions. It has been shown that it can be applied in vessels with short circulation times and low coalescing rates, that is, systems with a low dispersed phase volume fraction, in the presence of protective colloids (Park and Blair, 1975; Chatzi et al., 1989).

In the present study, the degree of inhomogeneity of the vessel content was assessed by collecting and measuring samples from three different positions in the reactor. It was found that the deviation of the average drop size, defined as $[(d_{32})_{max} - (d_{32})_{min}]/(d_{32})_{min}$, was always less than 6%, indicating that the degree of inhomogeneity could not be clearly differentiated from the experimental errors inherent in the measurement technique. For comparison, in a low dispersed phase system of styrene in water (Chatzi et al., 1989) the deviation of the average drop size between different sampling positions ranged from 1.2 to 7.6% and increased with increasing the dispersed phase volume fraction, Φ. For a system of methyl isobutyl ketone, (MIBK) in water Park and Blair (1975) found that the deviation was less than 5% for $\Phi = 0.005$ and more than 16% for $\Phi = 0.10$. For an isooctane-carbon tetrachloride in water system Mlynek and Reshnik (1972) reported changes of up to 5 and 29% for $\Phi \ll 0.10$ and $\Phi = 0.25$, respectively.

Effect of process variables on the drop-size distribution

Figure 3 illustrates the steady-state drop-size distributions obtained for a PVA concentration of 0.5 g/L, a dispersed phase volume fraction $\Phi = 0.50$, and agitation rates of 400, 450, 500, 600 and 700 rpm. The corresponding steady-state distributions for a PVA concentration of 1 g/L are shown in Figure 4. It is interesting to note that at high PVA concentrations (1 g/L, Figure 4), as the agitation rate increases the drop-size distribution shifts to smaller sizes and remains approximately the same for 550 and 700 rpm. On the other hand, at low PVA concentrations (0.5 g/L, Figure 3) the average drop size is originally decreased with impeller speed, followed by an increase at higher agitation rates (rpm > 500). This inversion is characteristic of the complex nature of the breakage and coalescence processes occurring in liquid-liquid dispersion systems. The results of Figure 4 are a manifestation of droplet coalescence dominating at increased intensity of turbulence above a certain value of agitation rate.

Indicative results showing the effect of PVA concentration on the steady-state drop-size distributions are depicted in

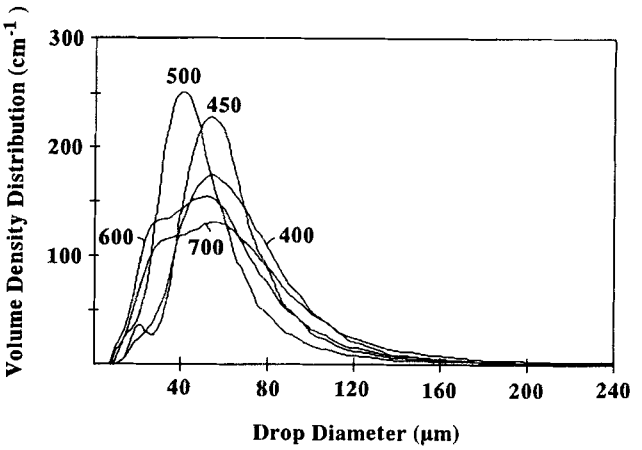

Figure 3. Effect of agitation rate on the steady-state drop-size distribution ([PVA] = 0.5 g/L).

Figures 5 and 6 for agitation rates of 400 and 700 rpm, respectively. As the interfacial tension decreases (PVA concentration increases) the drop-size distribution shifts to smaller sizes. At low agitation speeds (400 and 500 rpm), the drop breakage is the dominant mechanism affecting the drop-size distribution developments (Chatzi et al., 1991a). At high agitation speeds (700 rpm) drop coalescence becomes important, especially at lower PVA concentrations. Figure 7 illustrates the effect of agitation rate on the Sauter mean diameter for the two different PVA concentrations. At low stirring rates, the droplets in the suspension are very large. As the agitation rate increases, the droplet size originally decreases, it reaches a minimum value, and then starts increasing with agitation speed. A similar U-shape behavior has been reported in the literature (Johnson, 1980; Kelsall and Maitland, 1983; Tanaka and Hosogai, 1990) for suspension PVC particles. More specifically, it has been observed that this parabolic type of relationship is independent of the impeller size (Johnson, 1980) and that a family of curves is obtained, shifted to smaller diameters for higher concentrations of stabilizer (Kelsall and Maitland, 1983). The decreasing tendency of the droplet sizes with increasing impeller speed can be explained (Johnson, 1980; Kelsall and Maitland, 1983; Tanaka and

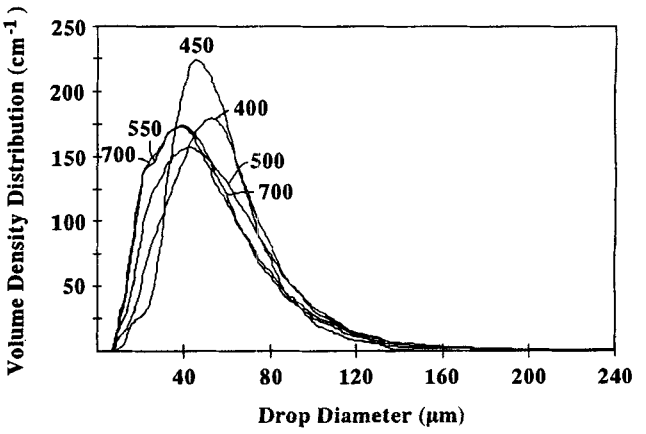

Figure 4. Effect of agitation rate on the steady-state drop-size distribution ([PVA] = 1 g/L).

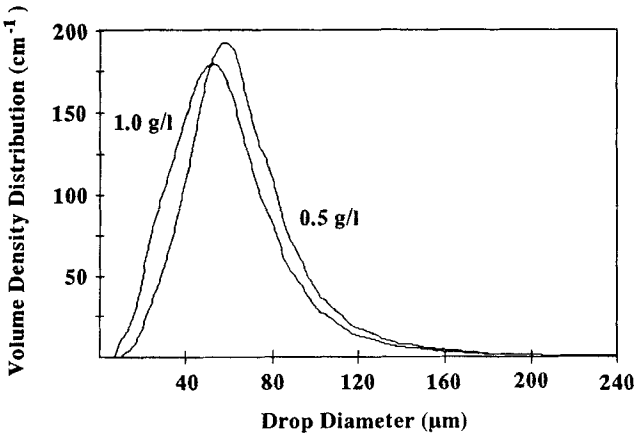

Figure 5. Effect of the PVA concentration on the steady-state drop-size distributions for an agitation rate of 400 rpm.

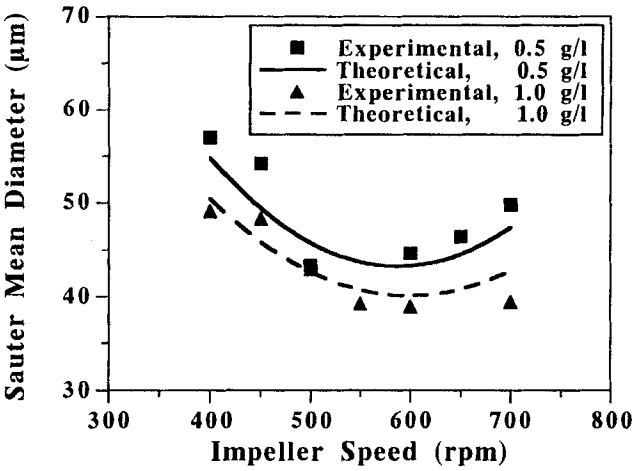

Figure 7. Dependence of the steady-state Sauter mean diameter on the agitation speed ([PVA]=0.5 and 1 g/L).

Hosogai, 1990) in terms of a higher breakage frequency. However, as the interfacial area increases due to the presence of a large number of small-size drops in the system, the effectiveness of the surfactant molecules on the interface begins to diminish, leading to coalescence/agglomeration and therefore, to a size increase of the droplets/polymerizing particles.

The interfacial tension between two immiscible liquids depends on the temperature and the type and concentration of surface active agents. In this study, the time variation of the interfacial tension of the butyl chloride–water system was measured over a wide range of PVA concentrations until the system reached equilibrium. Figure 8 depicts the effect of PVA concentration on the equilibrium interfacial tension for the system under investigation. It appears that at low PVA concentrations (< 0.001 g/L), the surface tension is relatively independent of the PVA concentration. At higher PVA concentrations the interfacial tension decreases almost linearly on a semilog scale. Finally, at very high PVA concentrations (> 0.1 g/L) the interfacial tension remains almost constant. This transition from a high to a low value of the interfacial tension has been reported in the literature and occurs in the PVA concentration range of 0.01 to 0.1 g/L, depending on the molecular weight of PVA and its molecular weight distribution, and it is characteristic of "hydrophilic" PVA molecules (PVA with a degree of hydrolysis greater than 90%). Peter and Fasbende (1964) reported that this transition coincides with a distinct change in the physicochemical properties of PVA solutions. The results of the present study indicate the existence of a similar transition for a "hydrophobic" PVA (such as degree of hydrolysis 73%) at lower concentration values (< 0.001 g/L). To our knowledge, this low concentration region has not been adequately studied for PVA having a low degree of hydrolysis. However, it is well recognized in the literature that the shape of the interfacial tension vs. concentration curve depends on the hydroxyl group content of the polyvinyl alcohol and, especially, on the numbers of adsorbed and unadsorbed PVA segments (Lankveld and Lyklema, 1972; Nilsson et al., 1985). For a paraffin-oil/water system in the presence of a "hydrophobic" PVA at concentrations greater than 0.001 g/L, it was found that the interfacial

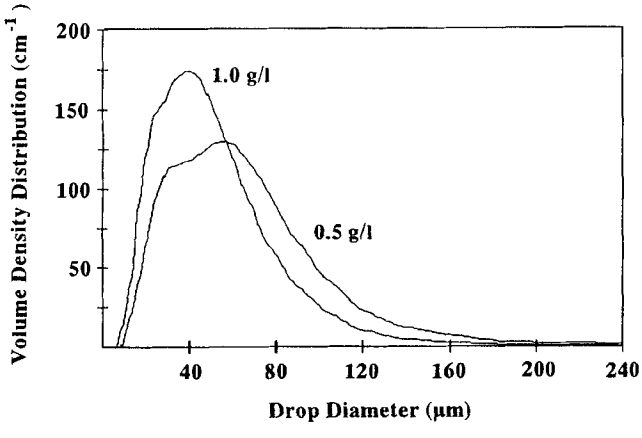

Figure 6. Effect of the PVA concentration on the steady-state drop-size distributions for an agitation rate of 700 rpm.

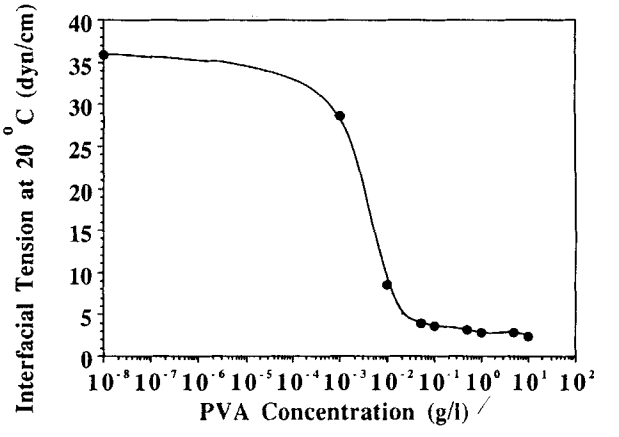

Figure 8. Dependence of the equilibrium interfacial tension of *n*-butyl chloride/water on the PVA concentration at 20°C.

tension decreased gradually following convex curves with respect to the PVA concentration. This decrease was more pronounced for lower molecular weight PVA, suggesting an increased surface affinity (Lankveld and Lyklema, 1972). A similar convex behavior is observed in this study at concentrations greater than 1 ppm (Figure 8).

An explanation for the observed variation of the interfacial tension with respect to the PVA concentration (Figure 8) has been proposed by Lankveld and Lyklema (1972) based on the dependence of interfacial tension on (1) the number of adsorbed polymer segments per unit area of the liquid-liquid interface, (2) the interaction free energy per segment in the loops of the adsorbed polymer molecules, and (3) the average loop length. The combined effects of segmental adsorption as well as loop interaction tend to decrease the interfacial tension due to the appearance of steric repulsion forces. These effects contribute to the surface activity of PVA. In the region of low PVA concentration, Zwick (1965) suggested that there might be a complete and rapid unfolding of the very flexible PVA molecules, resulting in an extended conformation of PVA with a large number of segments per molecule in the interfacial region. The break point marks the onset of almost complete coverage of the interface and its saturation with polymer molecules having an extended conformation. The rather steep decrease of interfacial tension at higher polymer concentrations is probably due to the increased adsorption of molecules and the appearance of strong loop repulsive forces. The conformation of the adsorbed molecules will be initially random. As the number of adsorbed segments increases, however, the packing of the molecules in the surface layer increases up to the formation of a monolayer. In the present study, the monolayer formation appeared at concentrations higher than 0.05 g/L for a "hydrophobic" grade PVA with a degree of hydrolysis 73% (Figure 8), as compared to 3 g/L measured for a more hydrophilic PVA (degree of hydrolysis 99%) (Chatzi et al., 1991b). Above this PVA concentration, the interfacial tension decreased by less than 0.5 dyn/cm.

In Figure 9 experimental measurements of the interfacial tension for the *n*-butyl chloride/water system at 20°C are plotted with respect to time for various PVA concentrations.

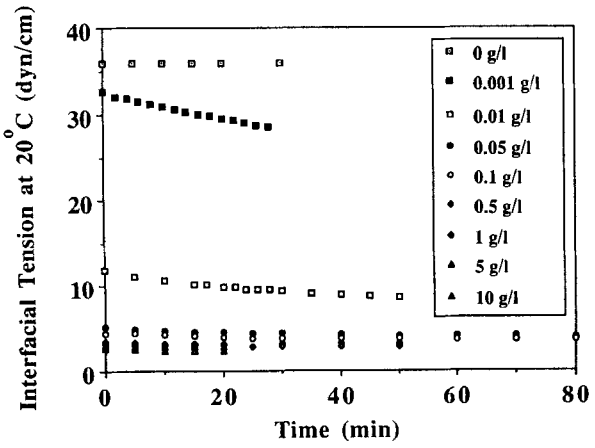

Figure 9. Time evolution of the interfacial tension of *n*-butyl chloride/water at 20°C for various PVA concentrations.

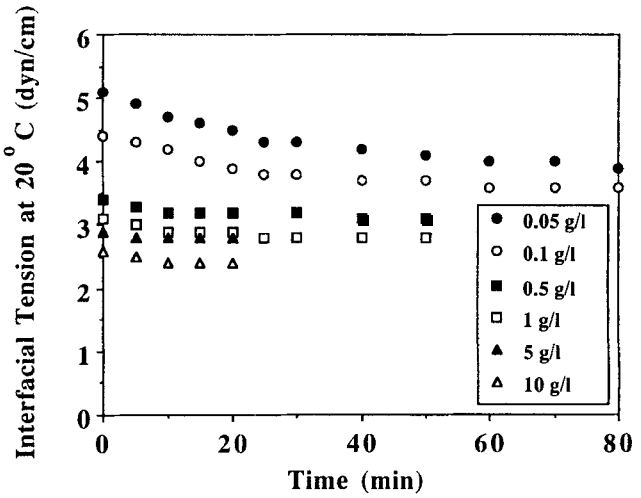

Figure 10. Time evolution of interfacial tension of *n*-butyl chloride/water at 20°C for PVA concentrations varying between 0.05 and 10 g/L.

The evolution of interfacial tension with time for the high PVA concentration is shown more clearly in Figure 10. It can be seen that as the PVA concentration increases, the time required for the system to reach equilibrium is reduced, indicating an increasing polymer diffusion rate to the liquid/liquid interface. Note that at a low PVA concentration (0.001 g/L) the initial interfacial tension value of 33 dyne/cm approaches that of the pure *n*-butyl chloride/water system (36 dyne/cm at 20°C).

As already discussed in this section, at low PVA concentrations the time dependence of interfacial tension is controlled by the diffusion of PVA molecules from the bulk phase to the interface, whereas at high PVA concentrations the time evolution of the interfacial tension is controlled by the reconformation of the polymer chains at the interface. Lankveld and Lyklema (1972) suggested that in the diffusion-control region the interfacial tension varies linearly with $t^{1/2}$, while $\partial\sigma/\partial t^{1/2}$ is proportional to the concentration of PVA within the limits of experimental error. Quantitative interpretation of the linear part of the $\sigma - t^{1/2}$ curve yields acceptable results, assuming that the decrease of interfacial tension is caused by the adsorption of a set of segments and not whole molecules. On the other hand, at high PVA concentrations the liquid-liquid interface is almost instantly covered by polymer molecules though not in the thermodynamically most favorable conformation. Equilibrium is approached, but not necessarily attained, by chain reconformation, which includes replacement of less surface active groups in the interface by more hydrophobic ones (such as acetate-containing blocks) and the rearrangement of loops. The rate of this type of reconformation process is believed to be proportional to the extent of deviation from the final situation (Lankveld and Lyklema, 1972). Hence an exponential decay is expected. Indeed, if the logarithm of $[\sigma(t) - \sigma(\infty)]/[\sigma(0) - \sigma(\infty)]$ is plotted against time, straight lines are obtained with correlation coefficients of 0.983 and 0.960, for two PVA concentrations of 0.05 and 0.1 g/L (Figure 11). This indicates an "instant" diffusion and reconformation-control of segments at the interface at high PVA concentrations (> 0.05 g/L). From the slope of these

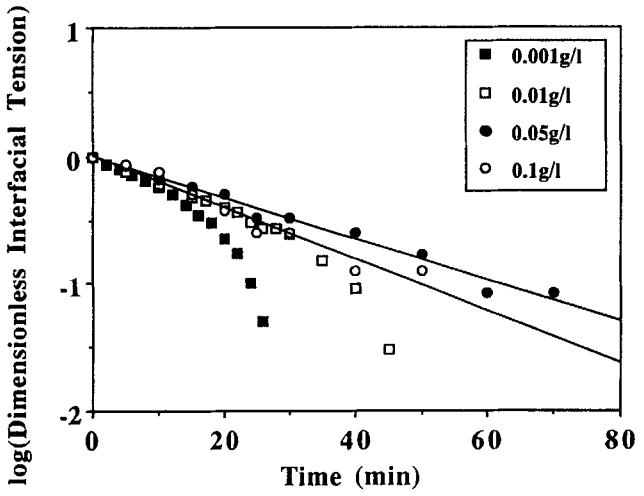

Figure 11. Time evolution of the dimensionless interfacial tension at 20°C and PVA concentrations varying between 0.001 and 0.1 g/L.

lines an average relaxation time of 55 min is calculated for the PVA molecules at the butyl chloride/water interface. An increased relaxation time at smaller PVA concentrations indicates a slower rate of reconformation. On the other hand, for the "low" PVA concentration region straight lines are obtained when interfacial tension is plotted against $t^{1/2}$ (Figure 12).

In a two-phase dispersion system, the drop-size distribution is determined by the relative contribution of breakage and coalescence mechanisms. Both processes are related to the drop surface energy, which is proportional to the interfacial tension and its evolution with time as a result of polymer concentration and conformation at the interface. The effect of stabilizer concentration on the steady-state drop-size distributions shown in Figures 5 and 6 are indicative of a larger contribution of coalescence at higher impeller speeds, espe-

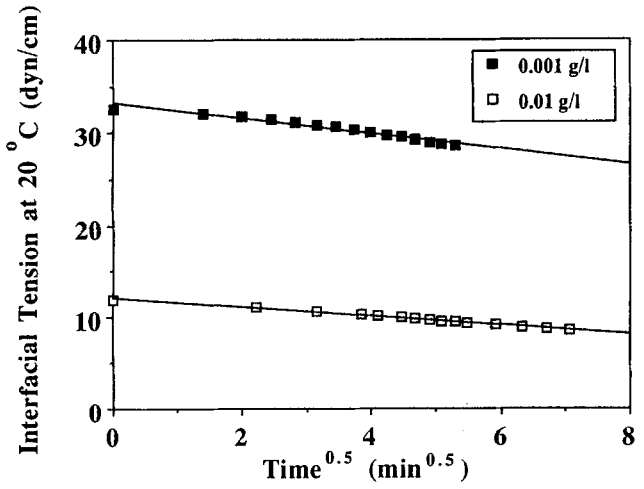

Figure 12. Variation of the interfacial tension of *n*-butyl chloride/water with the square root of time for two PVA concentrations (0.001 and 0.01 g/L) at 20°C.

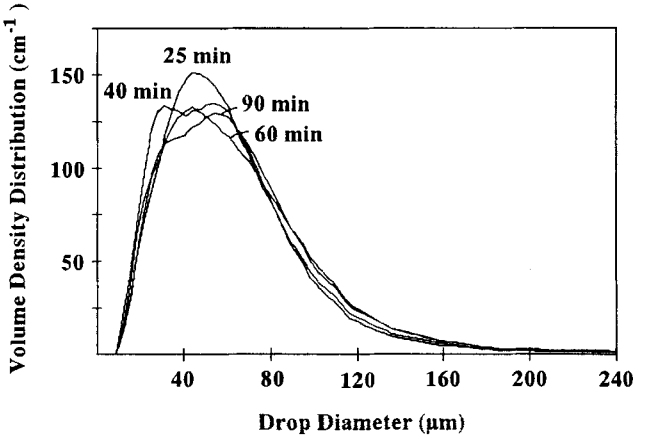

Figure 13. Time evolution of the volume density distribution ([PVA] = 0.5 g/L and 700 rpm).

cially, at the lower PVA concentrations. The calculated chain relaxation times indicate that PVA reconformation is faster at higher PVA concentrations, thus resulting in a more effective drop stabilization even at low agitation times. Indeed, Figures 13 and 14 show that at high PVA concentrations (1 g/L) limited drop coalescence is the controlling mechanism with increasing agitation time, but at low PVA concentrations (0.5 g/L) a more complicated time effect is observed. These results cannot be simply attributed to the slightly lower value of interfacial tension at high PVA concentrations, but they are rather a manifestation of the changing structure of PVA molecules at the interface and its complicated effect on the balance of breakage and coalescence rates at different agitation times.

Steady-State Population Balance Model

The dynamic behavior of a dispersion in an agitated tank and, therefore, its drop-size distribution are determined by the breakage and coalescence processes of the dispersed drops. If the dynamic character of breakage and coalescence is formulated, drop-size distribution can be predicted by the solution of the following population balance equation

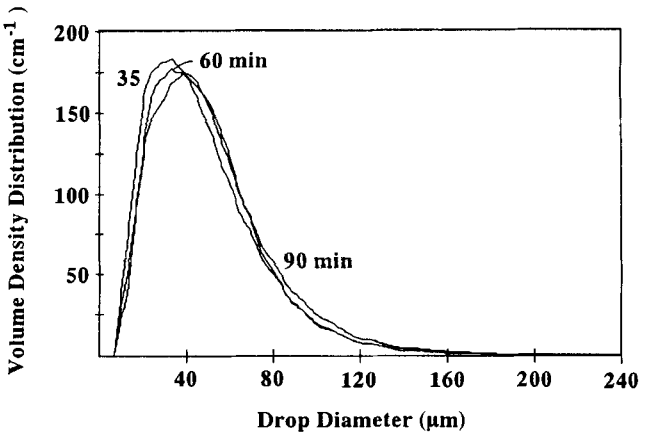

Figure 14. Time evolution of the volume density distribution ([PVA] = 1 g/L and 700 rpm).

(Valentas and Amundson, 1966; Valentas et al., 1966; Chatzi and Lee, 1987):

$$NA(d_v)[g(v)+\omega(v)] = (2/\pi)^{-1}(6/\pi)^{2/3}v^{2/3} \times \int_{d_v}^{d_{v_{max}}} \beta(v', v)u(v')g(v')NA(d_{v'})\, d(d_{v'}) + v^{2/3}\int_{d_{v_{min}}}^{d_{v/2}} (v-v')^{-2/3}\lambda(v-v', v')h(v-v', v') \times NA(d_{v-v'})NA(d_{v'})\, d(d_{v'}) \quad (1)$$

where

$$\omega(v) = \int_{d_{v_{min}}}^{d_{v_{max}-v}} \lambda(v, v')h(v, v')NA(d_{v'})\, d(d_{v'}). \quad (2)$$

Here N is the total number of drops in the vessel, $d_{v'}$, $d_{v-v'}$, ... denote the drop diameters corresponding to volumes v', $v-v'$, ..., respectively, and $A(d_v)\, d(d_v)$ is the number fraction of drops having diameter in the size range d_v to d_{v+dv}. Note that the diameter density function, $A(d_v)$, satisfies the normalization condition:

$$\int_{d_{v_{min}}}^{d_{v_{max}}} A(d_v)\, d(d_v) = 1. \quad (3)$$

Also, $g(v)$ is the fraction of drops having volume v that disappears through breakage per unit time, s^{-1}; $u(v')$ is the number of daughter droplets formed from breakage of one drop having volume v'; $\beta(v', v)$ denotes the number fraction of drops having volume v formed by breakage of a drop of volume v', cm^{-3}; $h(v, v')$ identifies the collision frequency of a drop having volume v with a drop of volume v', s^{-1}. Finally, $\lambda(v, v')$ is the coalescence efficiency given a collision of a drop having volume v with a drop of volume v'.

Note that all terms in Eq. 1 have dimensions $cm^{-1}s^{-1}$. Also the last integral is evaluated from $d_{v_{min}}$ to $d_{v/2}$ in order to avoid counting each coalescence event twice. The $d_{v_{min}}$ and $d_{v_{max}}$ appearing in the limits of the integrals correspond to the minimum and maximum droplet sizes present in the mixing vessel. The preceding model considerations are valid for an isothermal system with no interphase species transfer and chemical reactions occurring and for interaction frequencies independent of the droplet age. If we know the breakage and coalescence functions, Eqs. 1 and 2 can be solved numerically to calculate the steady-state drop-size distribution.

Breakage interaction frequency

Various generalized phenomenological breakage models have been proposed in the literature in order to relate the drop-size distribution with the basic hydrodynamics and physical properties of the system (Coulaloglou and Tavlarides, 1977; Narsimhan et al., 1979; Sovova, 1981; Chatzi et al., 1989; Chatzi and Kiparissides, 1992).

In general, the breakage interaction frequency of liquid-liquid dispersions is characterized by the transition probability of droplet breakage and the size distribution of the daughter droplets resulting from the breakage of the parent drop (Narsimhan et al., 1980). It has been postulated in the literature that breakup in turbulent fields may be caused by viscous shear forces, by turbulent pressure fluctuations (Hinze, 1955; Shinnar and Church, 1960), or by relative velocity fluctuations (Mikos et al., 1986; Narsimhan et al., 1979). Considering breakup by viscous shear forces, the droplet is first elongated into two fluid lumps separated by a thread or into a cylindrical thread and then breaks into two or more drops (Taylor, 1932, 1934; Sleichter, 1962; Karam and Bellinger, 1968; Narsimhan et al., 1980). On the other hand, since a droplet suspended in turbulent flow is exposed to local pressure and relative velocity fluctuations, it can be assumed that for nearly equal densities and viscosities of the two liquid phases, the droplet oscillates with the surrounding fluid. When the relative velocity is close to that required to make a drop marginally unstable, a number of small drops are stripped out from a larger one (Sleichter, 1962). This type of breakage is referred to as errosive breakage (Narsimhan et al., 1980). It is also possible that a transition in the type of deformation and breakage may take place, depending on the size of the droplet (Narsimhan et al., 1980).

Coulaloglou and Tavlarides (1977) developed a model for the two lumps-neck deformation and breakage of a drop in a turbulent flow field and derived the functional form of the breakage frequency, by assuming that (1) the turbulence is locally isotropic and (2) the size d of the breaking drops is within the size range of the inertial subrange eddies, $\eta < d < l_e$, where l_e may be interpreted as the average size of the energy containing eddies. The extent of the drop deformation and the turbulent kinetic energy transmitted to the drop by the turbulent eddies determine whether or not the drop will break or will return to its initial state. According to Coulaloglou and Tavlarides (1977), two different cases were distinguished:

Case 1. A drop of diameter d will break if its turbulent kinetic energy is greater than the drop surface energy. The breakage frequency is derived in terms of the fraction of drops with turbulent kinetic energy greater than a critical value and the time elapsed between the beginning of a drop deformation and its breakage (breakage time):

$$g(d) = C_1 N^* (D_1/d)^{2/3}(2/\pi) \times \Gamma\left\{3/2, C_{II}\sigma/\left[\rho_d (N^*)^2 D_1^{4/3} d^{5/3}\right]\right\}. \quad (4)$$

Case 2. Breakage of a drop is caused from a collision with a turbulent eddy. If the turbulent kinetic energy imparted to the drop is greater than the drop surface energy, the drop deforms and breaks. The breakage frequency is then determined by the fraction of these "energetic" collisions for a random motion of drops and eddies, and by the breakage time:

$$g(d) = C_1 N^* (D_1/d)^{2/3} \times \exp\left\{-C_{II}\sigma/\left[\rho_d (N^*)^2 (D_1)^{4/3} d^{5/3}\right]\right\}. \quad (5)$$

Case 3. Narsimhan et al. (1979) developed another model to describe the fragmentation of the droplet in a locally

isotropic flow field. Accordingly, the breakage of a droplet exposed to a turbulent field is due to its oscillation resulting from the relative velocity fluctuations due to the arrival of one or more eddies of different scale (frequency) at the surface of the droplet. The breakage frequency depends on the average number of eddies arriving at the surface of the drop per unit time (λ) and on the probability that an arriving eddy will have energy greater than or equal to the minimum increase in the surface energy required to break a droplet of diameter d. The parameter λ as a first approximation can be regarded as a constant and referred to as C_{VII}. The following expression of the breakage frequency has been derived by Narsimhan et al. (1979) for breakage into two equal-size drops:

$$g(d) = C_{\text{VII}} \operatorname{erfc}\left\{C_{\text{VIII}}(\sigma/\rho_d)^{1/2}/\left(d^{5/6}N^*(D_1)^{2/3}\right)\right\}. \quad (6)$$

The breakage process cannot be completely described, unless we know the distribution of the droplet sizes resulting from the breakage of a larger drop, $\beta(v', v)$, and the number of daughter drops per breakage, $\nu(v')$. The breakage distribution function can be assumed approximately normally distributed, since it is the combined result of a large number of independent random events.

For binary or thorough breakage of a parent drop of volume v', the daughter drops are normally distributed about a mean value $\bar{v}$ as

$$\beta(v', v) = (1/\sigma_v\sqrt{2\pi}) \exp\left[-(v-\bar{v})^2/2\sigma_v^2\right]. \quad (7)$$

Assuming that 99.6% of the droplets lie inside the interval $[\bar{v}-3\sigma_v, \bar{v}+3\sigma_v]$, then the standard deviation, σ_v, can be expressed as

$$\sigma_v = \frac{\bar{v}}{3} = \frac{v'}{3\nu(v')}. \quad (8)$$

A breakage distribution function was proposed by Chatzi et al. (1989) for errosive breakage, considering that a parent drop of volume v' breaks into N_{da} equal-volume (v_1) daughter drops and N_{sa} equal-volume (v_2) satellite drops with a fixed volume ratio $x = v_1/v_2$. The daughter drops are normally distributed and their size varies from $v_{\min}/[N_{da} + (N_{sa}/x)]$ till $v_{\max}/(N_{da} + (N_{sa}/x))$. The model was in principle similar to that proposed by Collins and Knudsen (1970) for turbulent pipe flow. The following expressions were derived (Chatzi et al., 1989) for the number of drops with volume v, $\nu(v')\beta(v', v)$, formed by breakage of a drop of volume v':

$$\nu(v')\beta(v', v) = \begin{cases} N_{da}\beta(v', v) + N_{sa}\beta(v', xv), & \text{if } v \le v'/(N_{da}x + N_{sa}) \quad (9) \\ N_{da}\beta(v', v), & \text{if } v'/(N_{da}x + N_{sa}) < v \le v'/[N_{da} + (N_{sa}/x)] \quad (10) \\ 0, & \text{if } v > v'/[N_{da} + (N_{sa}/x)]. \quad (11) \end{cases}$$

A modification of this model was introduced by Chatzi and Kiparissides (1992) considering that the number of satellite drops, N_{sa}, stripped out of the parent drop as well as the volume ratio of the daughter to the satellite drops, x, showed a linear dependence on the parent drop volume, with slopes $S_{N_{sa}}$ and S_x, respectively:

$$N_{sa} = 1 + \text{Int}[S_{N_{sa}} v_{pa}] \quad (12)$$

$$x = 1 + S_x v_{pa}. \quad (13)$$

The original breakage frequency equation (Eq. 6) derived by Narsimhan et al. (1979) assumed fragmentation corresponding to binary equal breakage. In the case of breakage into a number of daughter and satellite drops, Chatzi and Kiparissides (1992) showed that the parameter C_{VIII} could not be treated as a constant, but it had to be recalculated for each different breaking drop size according to:

$$C_{\text{VIII}} = C'_{\text{VIII}}\left[\frac{N_{da}x^{2/3} + N_{sa}}{(N_{da}x + N_{sa})^{2/3}} - 1\right]^{1/2} \quad (14)$$

where C'_{VIII} was an adjustable constant.

The modified breakage frequency and breakage distribution models developed by Chatzi et al. (1989, 1992) showed a unique ability to simulate the steady state as well as the dynamic behavior of bimodal drop-size distributions in low-coalescence and low holdup fraction liquid-liquid dispersion systems. Moreover, the proposed models could inherently take into account possible differences in the breakage characteristics of different-size drops. Thus, one satellite drop of size almost identical to the size of the daughter drop could be stripped off the very small-size parent drops, whereas a larger number of satellite drops of significantly smaller size could be stripped off the large-size parent drops.

Coalescence interaction frequency

Two models have been proposed in the literature to describe the coalescence of two drops in a turbulent flow field.

Shinnar and Church (1960) considered that two colliding drops may cohere together and be prevented from coalescing by a film of the continuous phase liquid trapped between them. Drainage of the film and subsequent coalescence is a result of attractive forces between the drops, usually of molecular nature, strong enough to cause drainage and rupture of the film separating the drops in a reasonable time. Coalescence may be prevented if the kinetic energy of the oscillations induced in the coalescing droplet pair due to turbulent pressure fluctuations is larger than the energy of adhesion between the drops. If the drops can be considered as deformable, which is generally true for low interfacial tension or large-size drops, the coalescence efficiency will be given according to Coulaloglou and Tavlarides (1977) as

$$\lambda_A(d_1, d_2) = \exp\left\{-C_{IV}\left[\mu_c \rho_c (N^*)^3 (D_I)^2/\sigma^2\right] \times [d_1 d_2/(d_1 + d_2)]^4\right\}. \quad (15)$$

If the drops behave like rigid spheres, the coalescence efficiency can be expressed as (Coulaloglou and Tavlarides, 1977)

$$\lambda_A(d_1, d_2) = \exp\left\{-C_{VI}\,\mu_c/\left[(N^*)(D_I)^{2/3}(d_1 + d_2)^{4/3}\right]\right\}. \quad (16)$$

The previous coalescence model does not take into account the possibility that a significant fraction of collisions results in immediate coalescence, occurring when the velocity of approach along the centerline of the drops at the instant of collision exceeds a critical value (Howarth, 1964). Sovova (1981) proposed an expression for the efficiency of collisions by considering that the drops follow the motion of eddies having a scale similar to their size. Drop coalescence occurs if the turbulent energy of collision of the drops is greater than their total surface energy. The fraction of "energetic collisions" has been derived as

$$\lambda_B(d_1, d_2) = \exp\left\{-C_V \sigma (d_1^2 + d_2^2)(d_1^3 + d_2^3)/\left[\rho_d (N^*)^2 (D_I)^{4/3} d_1^3 d_2^3 (d_1^{2/3} + d_2^{2/3})\right]\right\}. \quad (17)$$

Alternatively, coalescence may occur by a combination of both mechanisms (Sovova, 1981), yielding the following expression for the overall efficiency of collisions:

$$\lambda(d_1, d_2) = \lambda_A(d_1, d_2) + \lambda_B(d_1, d_2) - \lambda_A(d_1, d_2)\lambda_B(d_1, d_2). \quad (18)$$

The collision frequency has been derived by Coulaloglou and Tavlarides (1977) by assuming an analogy between collisions of molecules in the kinetic theory of gases and collisions of droplets in a locally isotropic flow field. For drops in the inertial subrange ($\eta < d < l_e$) the collision frequency is given by

$$h(d_1, d_2) = C_{III}(d_1^2 + d_2^2)(d_1^{2/3} + d_2^{2/3})^{1/2} N^* (D_I)^{2/3}. \quad (19)$$

Damping of turbulence

It has been reported in the literature (Coulaloglou and Tavlarides, 1977) that correlation of droplet-size distributions over a wide range of dispersed phase holdup fractions has to take into account the "damping" effects of the suspension on the local turbulence intensities at high holdup fractions. This can be approximated by an equation of the form:

$$\overline{u_\Phi^2} = (1 + \Phi)^{-2}\overline{u_{\Phi=0}^2} \quad (20)$$

where $\overline{u_\Phi^2}$ is the mean square of the relative velocity between two points separated by a distance d in the inertial subrange of turbulence, or the mean square fluctuation velocity of drops of diameter d:

$$\overline{u_\Phi^2} = K^3 \epsilon^{2/3} d^{2/3} \quad (21)$$

and ϵ is the energy dissipation per unit mass:

$$\epsilon = K'(N^*)^3 D^2. \quad (22)$$

Equation 20 should be considered in rederiving all breakage and collision frequency functions for high holdup fraction liquid-liquid dispersion systems. Eventually, the net "damping" effect of the dispersed phase on the intensity of turbulence can be expressed as a reduction of the effective agitation rate by a factor of $(1 + \Phi)$:

$$(N^*)_{\text{eff}} = \frac{N^*}{1 + \Phi}. \quad (23)$$

Theoretical Results and Discussion

The population balance equations (Eqs. 1 and 2) were solved for $A(d_v)$ using the normalization condition (Eq. 3). The total number of drops, N, was calculated from the following equation:

$$N = V_R \Phi \Big/ \int_{d_{v\min}}^{d_{v\max}} (\pi/6) d_v^3 A(d_v)\, d(d_v) \quad (24)$$

where V_R is the total volume of the dispersion and Φ the organic phase volume fraction.

The numerical solution of the integral Eq. 1 was obtained by approximating the integral terms using a composite Simpson's rule with a global error of $O(h^4)$, where h is the discretization step. For an even number of equally spaced intervals ("panels") the Simpson's 1/3 rule was applied, while for an odd number of panels Simpson's 3/8 rule was employed over the last three panels. One hundred equally spaced discretization points were used for the numerical integration. Thus, the nonlinear integral population balance (Eq. 1) was reduced to a set of nonlinear algebraic equations that were solved by an iterative technique. The convergence criterion of relative error between successive iterations was set to be less than 10^{-3}. The solution obtained was found to be independent of the diameter range used.

In simulating the experimentally measured steady-state drop-size distributions for the 1:1 by volume *n*-butyl chloride in water system, a variety of model combinations have been tested (models 4–14 for binary, thorough and erosive drop breakage, and models 15–18 for the drop coalescence). Selected models were judged by their ability to simulate the experimental distributions obtained for all sequences of impeller speeds and for the PVA concentrations tested. Experimental distributions were compared to theoretical predictions of diameter and volume density functions.

Previous experimental and theoretical studies of dynamic and steady-state drop-size distributions in dilute styrene/water systems (Chatzi et al., 1989; Chatzi and Kiparissides, 1992) revealed the applicability of Eq. 6 to vinyl monomer-

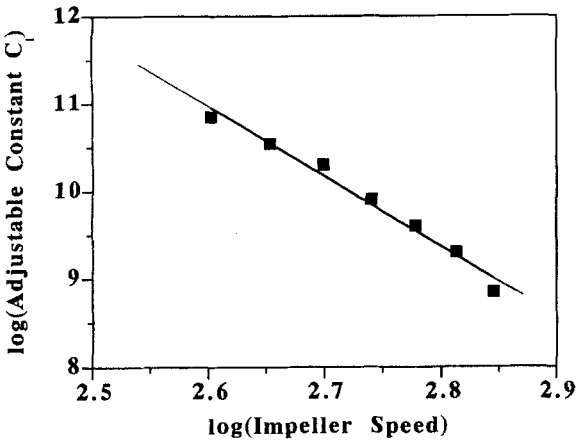

Figure 15. Dependence of the adjustable parameter C_1 on the agitation rate.

water dispersions. Equation 6 originally proposed by Narsimhan et al. (1979) considered droplet breakage to daughter and satellite drops as a result of oscillations due to relative velocity fluctuations. Despite the fact that the present geometry as well as the type and concentration of PVA were different from those employed by Narsimhan et al. (1979), it was found that the breakage model 6 could fit our experimental steady-state drop-size distributions reasonably well. The best fit to the complete set of experimental drop-size distributions for all impeller speeds and PVA concentrations was obtained by considering breakage of a parent drop into five daughter drops, and a number of equal-volume satellite drops. Note that the volume ratio of the daughter to the satellite drops as well as the number of satellite drops varied linearly with the parent drop volume. The modified expression of the model parameter C_{VIII}, Eq. 14, and the damping of the intensity of turbulence, Eq. 23, were also taken into account.

As shown in the experimental part of the article, it was observed that an increase in the intensity of turbulence (agitation rates greater than 600 rpm) resulted at larger droplet sizes. This is characteristic of the coalescence model introduced by Sovova (1981), which assumes an immediate drop coalescence when the velocity of approach along the center line of the drops at the instant of collision exceeds a critical value. However, coalescence by the mechanism of intervening film drainage may prevail at smaller agitation rates. Therefore, in our computer simulations we assumed a combination of both the Sovova model (Eq. 17) and the film drainage model. In the latter model, the expression for drops behaving as rigid spheres has been selected.

The estimated values of the model parameters are presented in Table 1. It should be pointed out that all model parameters except the lumped parameter $C_l = C_{VII}/C_{III}$ remain constant for all experimental conditions investigated. Only the parameter C_l decreases with increasing impeller speed as shown in Figure 15. However, the value of this parameter does not depend on the PVA concentration. The value of C_{VII} affects the breakage frequency, and indicates, in fact, the average number of eddies arriving at the surface of a drop per unit time, λ. According to the original derivation of breakage frequency by Narsimhan et al. (1979), λ is expected to depend both on the droplet diameter and the energy input per unit mass, $\bar{\epsilon}$. In the absence of *a priori* information about the dependence of λ on the drop diameter, it can be assumed independent of the drop size. Another assumption made in the original model derivation by Narsimhan et al. (1979) was a negligible effect of $\bar{\epsilon}$ on λ. A general expression of the energy input per unit mass, $\bar{\epsilon}$, for baffled and unbaffled systems is given by (Shuichi, 1958; Nishikawa et al., 1987):

$$\bar{\epsilon} = \frac{4K}{\pi} \frac{(N^*)^3 D_I^5}{D_T^2 H} \tag{25}$$

where P, $\bar{\epsilon}$, N^*, D_I, D_T, H, and K denote the power input (g·cm/s^2), the average power input/unit mass (cm^2/s^3), the impeller speed (s^{-1}), the impeller and tank diameters (cm), the tank height (cm), and the power number (dimensionless), respectively.

Therefore, the energy input per unit mass, $\bar{\epsilon}$, depends on the impeller speed and thus, the average number of eddies arriving on the surface of a drop per unit time, λ, is expected to show a dependence of the type

$$\lambda = K'(N^*)^{\alpha}.$$

Note that the adjustable parameter C_l exhibits a similar behavior according to the results of Figure 15.

The agreement between experimentally measured and predicted distributions is very satisfactory considering the various assumptions in formulating the interaction models and the inherent experimental errors. In Figures 16 to 19 experimental and theoretical volume density distributions, $A_v(d_v)$, are plotted for the two agitation speeds (400 and 700 rpm) and the two different PVA concentrations. The volume density distribution, $A_v(d_v)$, is defined as

$$A_v(d_v) = A(d_v)d_v^3 \Big/ \int_{d_{v_{min}}}^{d_{v_{max}}} A(d_v)d_v^3\, d(d_v). \tag{26}$$

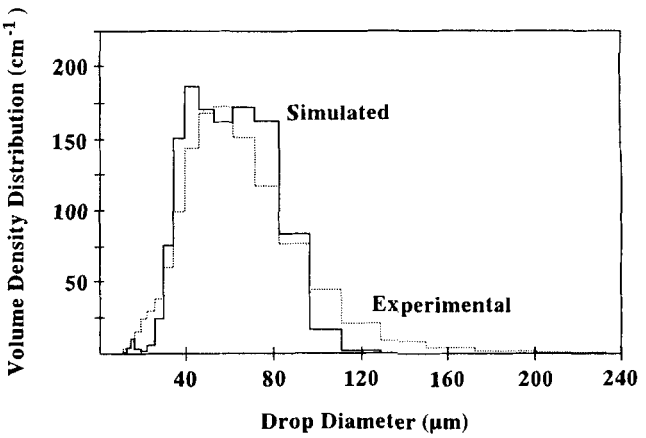

Figure 16. Comparison between experimental and predicted volume density distributions ([PVA]= 0.5 g/L and 400 rpm).

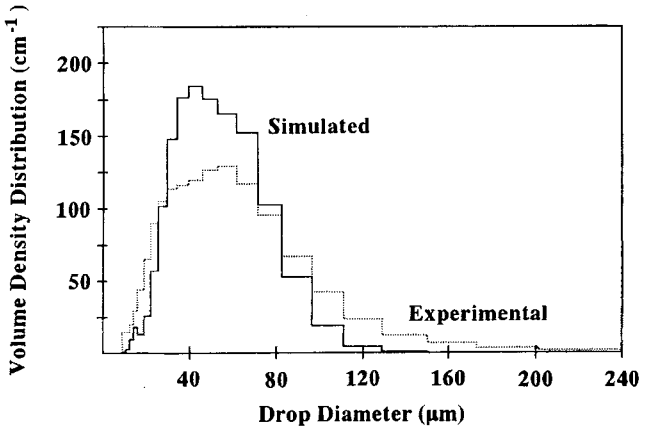

Figure 17. Comparison between experimental and predicted volume density distributions ([PVA]= 0.5 g/L and 700 rpm).

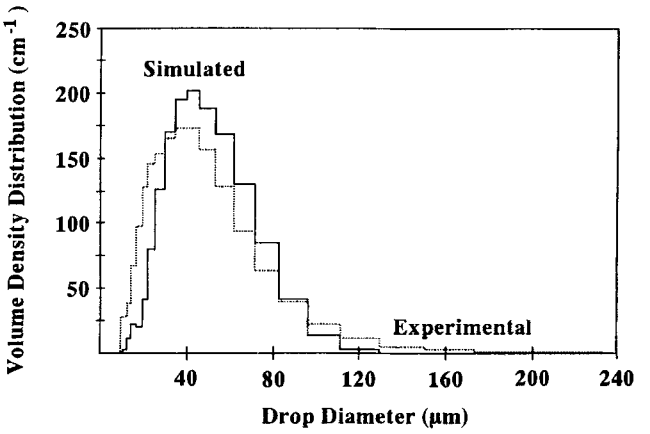

Figure 19. Comparison between experimental and predicted volume density distributions ([PVA]= 1 g/L and 700 rpm).

The continuous lines in Figures 16 to 19 represent the predicted distribution and the dotted lines represent the experimental ones. For comparison purposes, the simulation results have been transformed into a histogram similar to the experimental one. The model has the unique ability to simulate the complete set of steady-state drop-size distributions at different impeller speeds and PVA concentrations for the model system of butyl chloride in water. The predictive power of the proposed model has been further tested by plotting the theoretically calculated Sauter mean diameters as a function of the impeller speed (Figure 7). The model successfully describes the U-type behavior of the system for the lower concentration of PVA used (that is, 0.5 g/L), characteristic of a transition from a breakage- to a coalescence-dominated regime, depending on the combination of the degree of agitation and stabilization conditions. The agreement is quite satisfactory even at higher PVA concentrations considering the various assumptions in formulating the interaction models and the fact that exactly the same parameter values have been used for the simulation of drop-size distributions for both PVA concentrations.

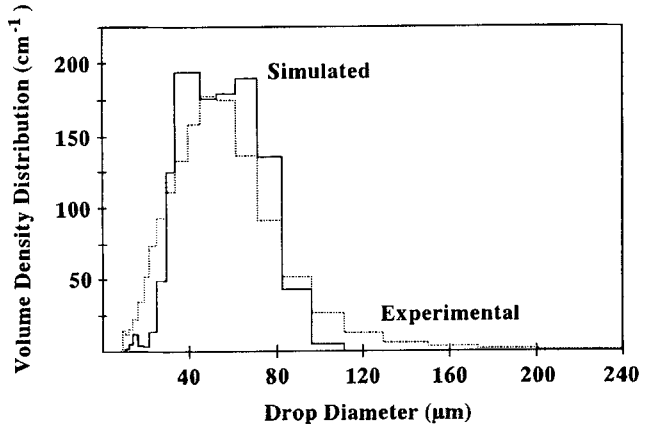

Figure 18. Comparison between experimental and predicted volume density distributions ([PVA]= 1 g/L and 400 rpm).

To our knowledge, no previous theoretical model predictions have reported illustrations of the U-type behavior of the Sauter mean diameter with respect to the impeller speed. Therefore, we believe that the present study is a step toward understanding and describing the mechanisms of breakage and coalescence in high holdup fraction dispersed phase systems, typically encountered in industrial suspension polymerization reactors.

Acknowledgment

The authors gratefully acknowledge Solvay S. A. for financially supporting this research.

Notation

d' = droplet diameters, cm
d_{32} = Sauter mean diameter, cm
μ_c = viscosity of the continuous phase, g/s·cm
ν_m = kinematic viscosity of the dispersion, cm^2/s
ρ_c = continuous phase density, g/cm^3
ρ_d = dispersed phase density, g/cm^3
σ = interfacial tension, dyn/cm

Literature Cited

Bürkholz, A., and R. Polke, "Laser Diffraction Spectrometers/Experience in Particle Size Analysis," *Part. Charact.*, **1**, 153 (1984).

Chatzi, E. G., and C. Kiparissides, "Dynamic Simulation of Bimodal Drop Size Distributions in Low-Coalescence Batch Dispersion Systems," *Chem. Eng. Sci.*, **47**, 445 (1992).

Chatzi, E. G., C. J. Boutris, and C. Kiparissides, "On-Line Monitoring of Drop Size Distributions in Agitated Vessels: 1. Effects of Temperature and Impeller Speed," *Ind. Eng. Chem. Res.*, **30**, 536 (1991a).

Chatzi, E. G., C. J. Boutris, and C. Kiparissides, "On-Line Monitoring of Drop Size Distributions in Agitated Vessels: 2. Effect of Stabilizer Concentration," *Ind. Eng. Chem. Res.*, **30**, 1307 (1991b).

Chatzi, E. G., A. D. Gavrielides, and C. Kiparissides, "Generalized Model for Prediction of the Steady-State Drop Size Distributions in Batch Stirred Vessels," *Ind. Eng. Chem. Res.*, **28**, 1704 (1989).

Chatzi, E. G., and J. M. Lee, "Analysis of Interactions for Liquid-Liquid Dispersions in Agitated Vessels," *Ind. Eng. Chem. Res.*, **26**, 2263 (1987).

Collins, S. B., and J. G. Knudsen, "Drop-Size Distributions Produced by Turbulent Pipe Flow of Immissible Fluids," *AIChE J.*, **16**, 1072 (1970).

Coulaloglou, C. A., and L. L. Tavlarides, "Description of Interaction Processes in Agitated Liquid-Liquid Dispersions," *Chem. Eng. Sci.*, **32**, 1289 (1977).
Hinze, J. O., "Fundamentals of the Hydrodynamic Mechanism of Splitting in Dispersion Processes," *AIChE J.*, **1**, 289 (1955).
Howarth, W. J., "Coalescence of Drops in a Turbulent Flow Field," *Chem. Eng. Sci.*, **19**, 33 (1964).
Johnson, G. R., "Effects of Agitation During VCM Suspension Polymerization," *J. Vinyl Technol.*, **2**, 138 (1980).
Karam, H. J., and J. C. Bellinger, "Deformation and Break-Up of Liquid Droplets in a Simple Shear Field," *Ind. Eng. Chem. Fund.*, **7**, 576 (1968).
Kelsall, D. G., and G. C. Maitland, "The Interaction of Process Conditions and Product Properties for PVC," *Polymer Reaction Engineering. Influence of Reaction Engineering on Polymer Properties*, K. H. Reichert and W. Greiseler, eds., Hansen, Vienna (1983).
Lankveld, J. M., and J. Lyklema, "Adsorption of Polyvinyl Alcohol on the Paraffin–Water Interface: I. Interfacial Tension as a Function of Time and Concentration," *J. Colloid Int. Sci.*, **41**, 454 (1972).
Mikos, A. G., C. G. Takoudis, and N. A. Peppas, "Reaction Engineering Aspects of Suspension Polymerization," *J. Appl. Pol. Sci.*, **31**, 2647 (1986).
Mlynek, Y., and W. Reshnick, "Drop Sizes in an Agitated Liquid-Liquid System," *AIChE J.*, **18**, 122 (1972).
Narsimhan, G., G. Gupta, and D. Ramkrishna, "A Model for Transitional Breakage Probability of Droplets in Agitated Lean Liquid-Liquid Dispersion," *Chem. Eng. Sci.*, **34**, 257 (1979).
Narsimhan, G., D. Ramkrishna, and J. P. Gupta, "Analysis of Drop Size Distributions in Lean Liquid-Liquid Dispersions," *AIChE J.*, **26**, 991 (1980).
Nilsson, H., C. Silvegren, and B. Törnell, "Suspension Stabilizers for PVC Production: I. Interfacial Tension Measurements," *J. Vinyl Technol.*, **7**, 112 (1985).
Nishikawa, M., F. Mori, S. Fujieda, and T. Kayama, "Scale-Up of Liquid-Liquid Phase Mixing Vessel," *J. Chem. Eng. Japan*, **20**, 454 (1987).
Park, J. Y., and L. M. Blair, "The Effect of Coalescence on Drop Size Distribution in an Agitated Liquid-Liquid Dispersion," *Chem. Eng. Sci.*, **30**, 1957 (1975).
Peter, S., and H. Fasbende, "Stromungsdoppelbrechung von Losungen Verschiedenartiger Polyvinylalkohole in Wassert in Salzlosungen," *Kolloid Z. Z. Poly.*, **196**, 125 (1964).
Shinnar, R., and J. M. Church, "Predicting Particle Size in Agitated Dispersions," *Ind. Eng. Chem.*, **52**, 253 (1960).
Shuichi, A., "Flow Patterns of Liquids in Agitated Vessels," *AIChE J.*, **4**, 485 (1958).
Sleichter, C. A., Jr., "Maximum Stable Drop Size in Turbulent Flow," *AIChE J.*, **8**, 471 (1962).
Sovova, H., "Breakage and Coalescence of Drops in a Batch Stirred Vessel: II. Comparison of Model and Experiments," *Chem. Eng. Sci.*, **36**, 1567 (1981).
Tanaka, M., and K. Hosogai, "Suspension Polymerization of Styrene with Circular Loop Reactor," *J. Appl. Pol. Sci.*, **39**, 955 (1990).
Taylor, G. I., "The Viscosity of a Fluid Containing Small Drops of Another Fluid," *Proc. R. Soc. London*, **A138**, 41 (1932).
Taylor, G. I., "The Formation of Emulsions in Definable Fields of Flow," *Proc. R. Soc. London*, **A146**, 501 (1934).
Valentas, K. J., and N. R. Amundson, "Breakage and Coalescence in Dispersed Phase Systems," *Ind. Eng. Chem. Fund.*, **5**, 533 (1966).
Valentas, K. J., O. Bilous, and N. R. Amundson, "Analysis of Breakage in Dispersed Phase Systems," *Ind. Eng. Chem. Fund.*, **5**, 271 (1966).
Voutetakis, S., "On the Design and Control of a Batch Polymerization Reactor," PhD Thesis, Chemical Engineering Dept., Aristotle Univ. of Thessaloniki, Thessaloniki, Greece (1992).
Zwick, M. M., "Poly(vinyl alcohol)-iodine Complexes," *J. Appl. Poly. Sci.*, **9**, 2393 (1965).

Manuscript received May 5, 1994, and revision received Sept. 15, 1994.